

Pan-Tissue Aging Clock Genes That Have Intimate Connections with the Immune System and Age-Related Disease

Adiv A. Johnson¹ and Maxim N. Shokhirev²

Abstract

In our recent transcriptomic meta-analysis, we used random forest machine learning to accurately predict age in human blood, bone, brain, heart, and retina tissues given gene inputs. Although each tissue-specific model utilized a unique number of genes for age prediction, we found that the following six genes were prioritized in all five tissues: *CHI3L2*, *CIDEA*, *FCGR3A*, *RPS4Y1*, *SLC11A1*, and *VTCN1*. Since being selected for age prediction in multiple tissues is unique, we decided to explore these pan-tissue clock genes in greater detail. In the present study, we began by performing over-representation and network topology-based enrichment analyses in the Gene Ontology Biological Process database. These analyses revealed that the immunological terms “response to protozoan,” “immune response,” and “positive regulation of immune system process” were significantly enriched by these clock inputs. Expression analyses in mouse and human tissues identified that these inputs are frequently upregulated or downregulated with age. A detailed literature search showed that all six genes had noteworthy connections to age-related disease. For example, mice deficient in *Cidea* are protected against various metabolic defects, while suppressing *VTCN1* inhibits age-related cancers in mouse models. Using a large multitissue transcriptomic dataset, we additionally generate a novel, minimalistic aging clock that can predict human age using just these six genes as inputs. Taken all together, these six genes are connected to diverse aspects of aging.

Keywords: aging clock, machine learning, age prediction, random forest, age-related disease, aging

Introduction

IN 2013, BOTH HORVATH¹ and Hannum et al.² utilized a panel of methylated CpG sites in conjunction with a regression model to predict human age. Such computational models are commonly referred to as aging clocks,³ and it is becoming increasingly well-established that the disparity between predicted age and chronological age often correlates with various health parameters^{4,5} and lifestyle choices.^{6,7} A recent study, for example, found that epigenetic age is a better predictor of mortality than the well-established frailty index.⁸ These aging clocks are capable of measuring biological age, which is a useful metric that differentiates between the passage of time and an individual's internal rate of biological aging.^{9,10} How rapidly or slowly an individual ages varies greatly¹⁰ and is dependent on a combination of genetic,¹¹ environmental,¹² and behavioral¹³ factors. Computational age predictors are also sensitive to pharmacological inter-

ventions in worms,¹⁴ mice,¹⁵ and humans.¹⁶ Both molecular and nonmolecular inputs can be utilized for age prediction, such as methylated CpG sites,¹ genes,¹⁷ transcriptional elements,¹⁸ microRNAs,¹⁹ proteins,⁶ ions,²⁰ metabolites,²¹ frailty index scores,¹⁵ and anatomical photographs.²² For more detailed information on aging clocks, we recommend two excellent reviews by Galkin et al.³ and Bell et al.²³

Recently, we developed a series of novel transcriptomic aging clocks in both multitissue and tissue-specific human datasets.¹⁷ As part of this prior study, we used random forest machine learning to identify gene sets that can predict age in blood, bone, brain, heart, and retina tissue. We chose random forest for regression training because it outperformed several other models for age prediction. Although each tissue-specific clock used at least 200 important genes for age prediction (*e.g.*, there were 262 important genes for the blood clock and 390 important genes for the brain clock), only the following six genes were commonly utilized across

¹Independent Researcher, Tucson, Arizona, USA.

²Razavi Newman Integrative Genomics and Bioinformatics Core, Salk Institute for Biological Studies, La Jolla, California, USA.

all five tissues: *CHI3L2*, *CIDEA*, *FCGR3A*, *RPS4Y1*, *SLC11A1*, and *VTCN1*.¹⁷ Since being prioritized and deemed important for transcriptomic age prediction in five different tissues is unique, we decided to explore these six genes in more detail to better understand their connection to aging.

Existing evidence hints that these genes may play an important role in the aging process. Since various aspects of lipid metabolism directly regulate life span and age-related disease,²⁴ it is interesting that *CIDEA* is an important regulator of lipid metabolism.²⁵ *FCGR3A* is a gene expressed by natural killer cells²⁶ that is also upregulated in human retinal pigment epithelial cells derived from older donors.²⁷ One of the CpG sites used to generate Horvath's seminal pan-tissue epigenetic aging clock is associated with the gene *CHI3L2*,¹ which encodes for a secreted glycoprotein that has been linked to cartilage homeostasis.²⁸ While the specific function of *RPS4Y1* is elusive, this gene encodes a ribosomal protein and has been associated with aging-relevant processes such as fat deposition²⁹ and resistance to anti-inflammatory drugs.³⁰ *SLC11A1* is a metal ion transporter that responds to various types of infection³¹ and is down-regulated in periodontal ligament stem cells derived from older individuals.³² *VTCN1* is a regulator of T cell immunity³³ and a driver of age-related cancer in mice.³⁴

In this study, we delve into these six genes in considerable detail. We do this by performing enrichment analyses, analyzing expression changes with age in multiple mouse and human tissues, and performing a targeted literature search. While performing these expression analyses, we additionally identify a panel of six microRNAs that undergo significant concentration shifts in different human tissues. Moreover, we show that these six genes can be used to predict age in a large multitissue dataset. Our results indicate that *CHI3L2*, *CIDEA*, *FCGR3A*, *RPS4Y1*, *SLC11A1*, and *VTCN1* are intimately connected to different aspects of aging.

Results

Over-representation and network topology-based enrichment analyses highlight the immune system

In our previous work, we identified the following six genes that were important for transcriptomic age prediction in blood-, bone-, brain-, heart-, and retina-specific aging clocks: *CHI3L2*, *CIDEA*, *FCGR3A*, *RPS4Y1*, *SLC11A1*, and *VTCN1*.¹⁷ To better understand the function of these pan-tissue clock inputs, we first performed enrichment analyses in the Gene Ontology Biological Process database.³⁵ The Gene Ontology Resource contains a vast array of information pertinent to gene function and can be used to understand what biological processes are associated with a group of genes or proteins.³⁵ Gene names, protein names, and UniProt IDs for each of these inputs are provided in Table 1. A term was deemed significantly enriched if it had a false discovery rate (FDR) <0.05.

The top 10 results from our over-representation analysis (Fig. 1) were "response to protozoan," "interleukin-2 production," "interferon-gamma production," "phagocytosis," "leukocyte proliferation," "RNA catabolic process," "adaptive immune response," "immune response-regulating signaling pathway," "T cell activation," and "positive regulation of cytokine production." Of these, the only significantly enriched term was "response to protozoan." Since we only

TABLE 1. THE GENE NAME, PROTEIN NAME, AND UNIPROT ID ARE PROVIDED FOR SIX GENES THAT WERE PREVIOUSLY SHOWN TO BE IMPORTANT FOR TRANSCRIPTOMIC AGE PREDICTION IN HUMAN BLOOD, BONE, BRAIN, HEART, AND RETINA

Gene name	Protein name	UniProt ID
<i>CHI3L2</i>	Chitinase-3-like protein 2	Q15782
<i>CIDEA</i>	Cell death activator CIDE-3	Q96AQ7
<i>FCGR3A</i>	Low affinity immunoglobulin gamma Fc region receptor III-A	P08637
<i>RPS4Y1</i>	40S ribosomal protein S4, Y isoform 1	P22090
<i>SLC11A1</i>	Natural resistance-associated macrophage protein 1	P49279
<i>VTCN1</i>	V-set domain-containing T cell activation inhibitor 1	Q7Z7D3

had a small number of genes to analyze, we expanded the enrichment network to include the top 50 neighbors using a separate network topology-based enrichment analysis. The expansion was done in the BioGRID database, which is a resource that houses information about chemical, genetic, and protein interactions.³⁶ This approach identified two terms that were significantly enriched: "immune response" and "positive regulation of immune system process" (Fig. 2). With the exception of "phagocytosis" and "RNA catabolic process," all of these results overtly highlight the immune system. Given that phagocytosis is an integral immune process,³⁷ the "phagocytosis" enrichment term may also be immunologically relevant. The other nonimmunological result of "RNA catabolic process" is relevant to genomic regulation. This is worth mentioning since genomic instability is a canonical hallmark of aging.³⁸

We proceeded to more closely examine these clock inputs by collating all of their known annotations in the Gene Ontology database (Table 2). The most prevalent theme implicated by these annotations was again the immune system, with annotations relevant to the immune system being linked with *FCGR3A*, *RPS4Y1*, *SLC11A1*, and *VTCN1*. Examples of immunological annotations include "IgG binding" (linked with *FCGR3A*), "viral transcription" (linked with *RPS4Y1*), "inflammatory response" (linked with *SLC11A1*), and "adaptive immune response" (linked with *VTCN1*).

Cidec and *Slc11a1* increase their expression level with age in multiple mouse tissues

Previously, Schaum et al. used bulk RNA sequencing to examine how genes vary with age in 17 different mouse organs.³⁹ Although *Chi3l2*, *Fcgr3a*, and *Rps4y1* were not measured under these names in this dataset, the genes *Cidec*, *Slc11a1*, and *Vtcn1* were measured in multiple mouse organs. By comparing the expression of these genes in mice aged 24 months to younger 3-month-old mice, we found that both *Cidec* and *Slc11a1* undergo significant (FDR <0.05) expression shifts with age. Specifically, the expression of *Cidec* increases in bone (Fig. 3A) and liver (Fig. 3B), while *Slc11a1* becomes overexpressed in brain (Fig. 3C), gonadal fat (Fig. 3D), kidney (Fig. 3E), and lung (Fig. 3F).

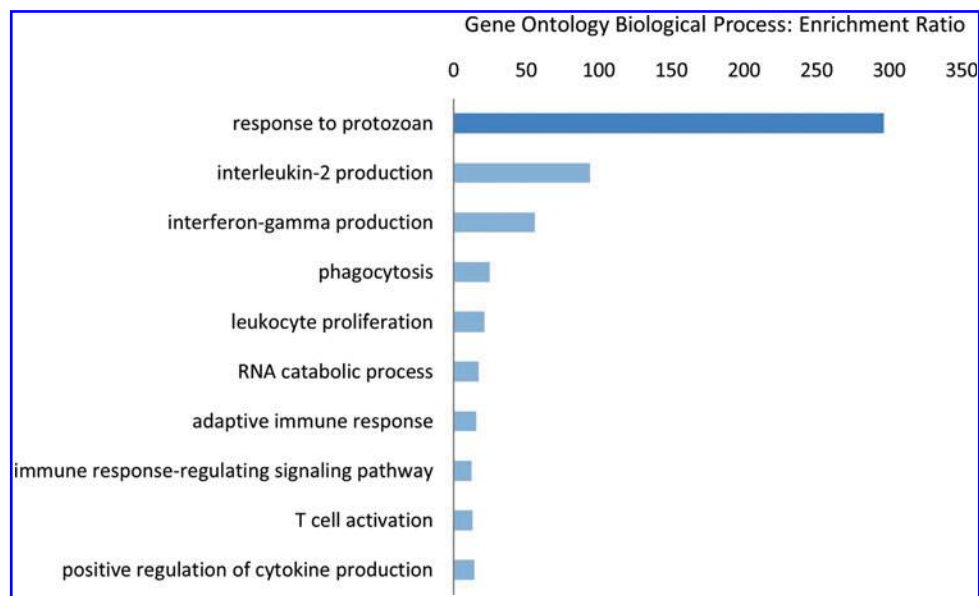


FIG. 1. Over-representation analysis in the Gene Ontology Biological Process database. To better understand what biological processes are associated with the six transcriptomic clock genes (*CHI3L2*, *CIDEA*, *FCGR3A*, *RPS4Y1*, *SLC11A1*, and *VTCN1*), we visualize the 10 most enriched results and organize them by enrichment ratio. The significant enrichment term in dark blue has a FDR < 0.05, while the nonsignificant enrichment terms in light blue have a FDR > 0.05. FDR, false discovery rate. Color images are available online.

CHI3L2, *FCGR3A*, *SLC11A1*, and *VTCN1* change their expression level with age in human tissue

Using the human transcriptomic data that we collated in our previous study,¹⁷ we next assessed whether or not these six pan-tissue clock genes significantly change their expression level with age in different human tissues. We performed a differential expression analysis to compare expression between older adults (≥70 years) and younger adults (30–69 years) in blood (Supplementary Table S1), brain (Supplementary Table S2), heart (Supplementary Table S3), and retina (Supplementary Table S4). In the blood transcriptomic dataset, there were 178 samples with an age range of 30–73 years. The brain, heart, and retina transcriptomic datasets included 91 samples (32–99 years), 151 samples (33–83 years), and 176 samples (47–95 years), respectively.

This analysis revealed that *CHI3L2*, *FCGR3A*, *SLC11A1*, and *VTCN1* significantly change their expression level with age in at least one tissue (Table 4). *CHI3L2* is downregulated in blood and upregulated in the brain and retina. *FCGR3A* increases its expression level in brain tissue, while *SLC11A1* is downregulated in blood and upregulated in the brain. *VTCN1* is diminished in brain tissue derived from older adults. Both *CIDEA* and *RPS4Y1* did not significantly change their expression level with age in blood, brain, heart, or retina (Table 4). Interestingly, our data indicate that *SLC11A1* in the brain is increased with age in both humans (Table 4) and mice (Table 3).

Surprisingly, the following six microRNAs were significantly differentially expressed with age in all four tissues: MIR100, MIR10B, MIR191, MIR21, MIR222, and MIR27B (Supplementary Table S5). This is quite intriguing as various microRNAs have been shown to regulate life span in model organisms.^{40,41} There were 26 genes that were significantly upregulated or downregulated in at least three tissues, and one of these was *CHI3L2* (Supplementary Table S5).

In human plasma, the protein expression of CHI3L2 becomes destabilized with age

We next explored whether any of these clock inputs were available for measurement in a plasma proteomic dataset derived from 4263 healthy individuals aged 18–95 years.⁴ Of the six pan-tissue clock inputs, only *CHI3L2* was measured in this large dataset. *CHI3L2* had a q.Age (*i.e.*, how significantly a given protein changes its expression level with age) of 0.015 and a Coefficient.Age (*i.e.*, whether a protein trends toward increased or decreased expression with age) of −0.00033. Thus, this protein significantly changes its expression level with age in human plasma and trends toward a decreased expression level over time. A close examination of how this protein's expression changes with age (Fig. 4) shows that, from the age of 18 years to ~65 years, its expression level is relatively stable. After ~65 years of age, the expression of *CHI3L2* becomes markedly destabilized with some individuals exhibiting either sharp increases or decreases in expression (Fig. 4). The gene expression of *CHI3L2* also decreases with age in human blood (Table 4).

All six clock genes exhibit tangible connections to age-related disease

We were also curious whether or not these aging clock inputs have known connections to age-related disease. After performing a literature search, we provide connections palpably pertinent to age-related disease for each gene in Table 5.

Suggestive of a more direct role in the regulation of age-related disease, arthritis in mice is induced through treatment with recombinant *CHI3L2*.⁴² Mice deficient in *Cidec* are resistant to diet-induced insulin resistance and weight gain⁴³ and, in a rat model of diabetic cardiomyopathy, silencing *Cidec* improves cardiac function.⁴⁴ The progression of atherosclerotic lesions in *Ldlr*^{−/−} mice is inhibited by

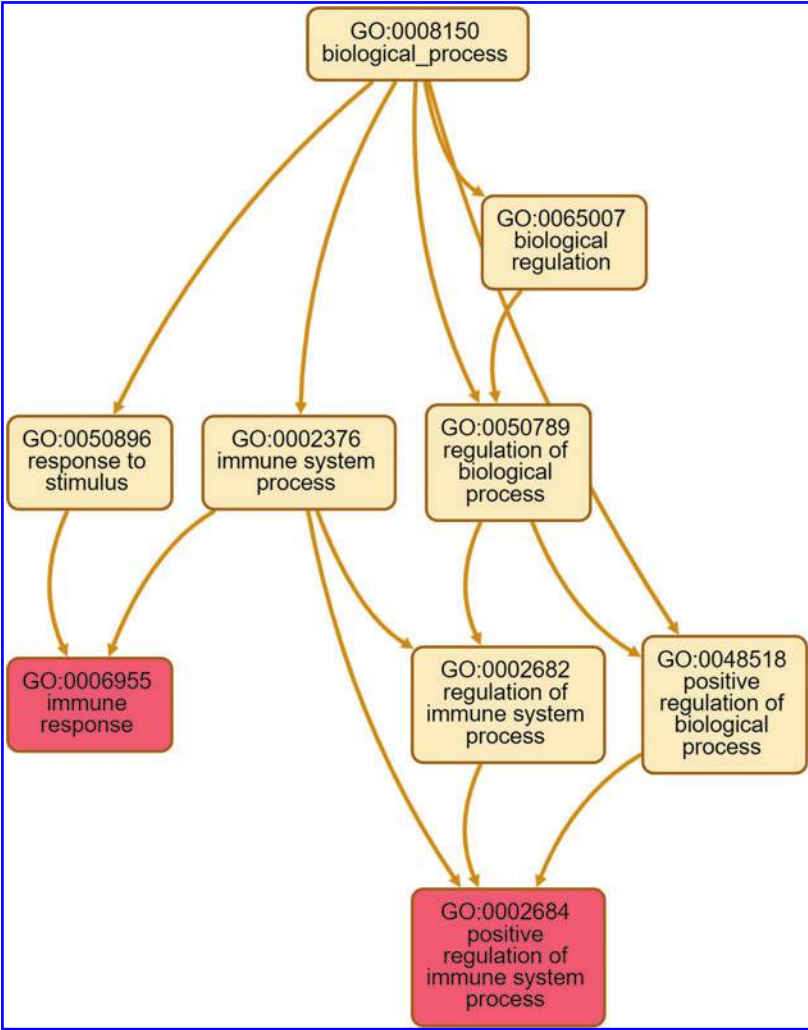


FIG. 2. Network topology-based analysis using the PPI BioGRID network for expansion. Over-represented Gene Ontology Biological Process terms are visualized as a dendrogram with the two significantly enriched terms “immune response” and “positive regulation of immune system process” highlighted in red. The ancestors of these two enriched terms (*i.e.*, “biological process,” “response to stimulus,” “immune system process,” “biological regulation,” “regulation of biological process,” “regulation of immune system process,” and “positive regulation of biological process”) are shown in beige. Color images are available online.

the deletion of *Fcgr3a*,⁴⁵ and the number of tumor modules is decreased by the deletion of *Vtcn1* in a mouse model of breast cancer.⁴⁶ Additional *in vivo* mouse studies indicate that genetically deleting *Cidec* promotes beneficial metabolic effects,^{47,48} creating a deficiency in *Slc11a1* delays wound healing,⁴⁹ inducing a mutation in *Slc11a1* exacerbates chemically-induced arthritis,⁵⁰ and suppressing VTCN1 inhibits cancer.^{51,52} Collectively, these genes have been reported to be differentially expressed in amyotrophic lateral sclerosis,⁵³ Alzheimer’s disease,⁵⁴ Parkinson’s disease,⁵⁵ and mild cognitive impairment.⁵⁶ They have also been used to predict prognosis in patients with renal cell carcinoma,⁵⁷ glioblastoma multiforme,⁵⁸ oral squamous cell carcinoma,⁵⁹ thyroid cancer,⁶⁰ hepatocellular carcinoma,⁶¹ and prostate cancer.⁶² A full list of literature connections relevant to age-related disease—five for each pan-tissue clock gene—can be found in Table 5.

A novel age predictor that exclusively utilizes these six genes as inputs

Given that these genes were all utilized for age prediction by five different tissue-specific age predictors,¹⁷ we decided to test the ability of these six genes to predict age in a multitissue transcriptomic dataset that we previously collated and filtered, which includes 3060 high-quality RNA-Seq samples spanning different tissues and representing both healthy and unhealthy individuals.¹⁷ Using random forest machine learning in conjunction with these six genes as inputs, we used a 10-fold cross validation approach to generate a Pearson correlation (R) of 0.76 and a root-mean square error (RMSE) of 9.77 years (Fig. 5). While not as accurate as our previous age predictors that utilized a larger number of inputs,¹⁷ these results demonstrate that an

TABLE 2. ASSOCIATED GENE ONTOLOGY ANNOTATIONS ARE PROVIDED FOR EACH CLOCK INPUT LISTED IN TABLE 1

Gene name	Gene ontology annotations
<i>CHI3L2</i>	Carbohydrate binding; carbohydrate metabolic process; chitin binding; chitin catabolic process; chitinase activity; extracellular region; extracellular space
<i>CIDEA</i>	Apoptotic process; cytosol; endoplasmic reticulum; execution phase of apoptosis; lipid droplet; lipid droplet organization; molecular function; nucleus; protein binding; regulation of apoptotic process
<i>FCGR3A</i>	Cell surface receptor signaling pathway; external side of plasma membrane; extracellular exosome; Fc-gamma receptor signaling pathway involved in phagocytosis; IgG binding; immune response; integral component of plasma membrane; plasma membrane; regulation of immune response; transmembrane signaling receptor activity
<i>RPS4Y1</i>	Cytosol; cytosolic small ribosomal subunit; membrane; multicellular organism development; nuclear-transcribed mRNA catabolic process, nonsense-mediated decay; nucleoplasm; nucleus; polysome; protein binding; RNA binding; rRNA binding; SRP-dependent cotranslational protein targeting to membrane; structural constituent of ribosome; translation; translational initiation; viral transcription
<i>SLC11A1</i>	Activation of protein kinase activity; antigen processing and presentation of peptide antigen; antimicrobial humoral response; cadmium ion transmembrane transport; cadmium ion transmembrane transporter activity; cell redox homeostasis; cellular cadmium ion homeostasis; cellular iron ion homeostasis; defense response to bacterium; defense response to Gram-negative bacterium; defense response to protozoan; ficolin-1-rich granule membrane; inflammatory response; integral component of plasma membrane; iron ion homeostasis; iron ion transmembrane transport; iron ion transmembrane transporter activity; iron ion transport; L-arginine transport; late endosome; late endosome membrane; lysosome; macrophage activation; manganese ion transmembrane transport; manganese ion transmembrane transporter activity; manganese ion transport; metal ion export; metal ion:proton antiporter activity; MHC class II biosynthetic process; mRNA stabilization; multicellular organismal iron ion homeostasis; negative regulation of cytokine production; neutrophil degranulation; nitrite transport; phagocytic vesicle membrane; phagocytosis; plasma membrane; positive regulation of cytokine production; positive regulation of dendritic cell antigen processing and presentation; positive regulation of gene expression; positive regulation of interferon-gamma production; positive regulation of phagocytosis; positive regulation of T-helper 1 type immune response; positive regulation of transcription by RNA polymerase II; protein homodimerization activity; respiratory burst; response to bacterium; response to interferon-gamma; response to lipopolysaccharide; T cell proliferation involved in immune response; tertiary granule membrane; transition metal ion transmembrane transporter activity; vacuolar acidification; wound healing
<i>VTCN1</i>	Adaptive immune response; external side of plasma membrane; integral component of membrane; molecular function; negative regulation of apoptotic process; negative regulation of T cell activation; negative regulation of T cell proliferation; regulation of cytokine production; signaling receptor binding; T cell receptor signaling pathway

ultraminimalistic transcriptomic age predictor can be constructed using a very small number of genes as inputs.

Since the set of healthy transcriptomes that we previously collated spans multiple datasets, we were curious how well this model performed in different tissues. It was able to predict age in adipose (Fig. 6A), blood (Fig. 6B), bone (Fig. 6C), brain (Fig. 6D), heart (Fig. 6E), liver (Fig. 6F), lung (Fig. 6G), and retina (Fig. 6H). Across all eight tissues, the *R* ranged from 0.85 to 0.98, while the RMSE varied from 1.58 to 6.49 years (Fig. 6). The adipose ($n=374$), blood ($n=178$), retina ($n=176$), heart ($n=151$), brain ($n=91$), bone ($n=89$), liver ($n=44$), and lung ($n=25$) tissues each represented a unique number of transcriptomes that were analyzed.

While these results are interesting, the ability of this clock to accurately predict age in different tissues is not surprising given that they are part of the same dataset the machine learning model was trained on. Thus, we sought to test the generalizability of this clock in a novel independent dataset. To do this, we measured age in 144 transcriptomes (age range of 38–103 years) derived from human brain tissue (Fig. 7). While our clock was significantly correlated with age (p -value=0.0036), the accuracy was lower with an *R* of 0.23 and a RMSE of 27.29 (Fig. 7). Our interpretation of these data is that, to generate a more robustly generalizable

age predictor using just these six genes, a much larger collection of RNA-seq data would be required. Alternatively, the inclusion of additional gene inputs may be needed to make this more broadly applicable.

Discussion

In this study, we thoroughly explore the relationship between six pan-tissue aging clock genes and different aspects of aging. As part of this work, we visualize how the expression of *CHI3L2* changes over time in a large proteomic dataset derived from human plasma. A closer analysis of this plot shows that the expression of this protein remains relatively stable during the majority of adulthood. However, starting around 65 years of age, individuals begin to exhibit prominent alterations in expression. While this overall leads to a decreased expression level over time, some individuals exhibit sharp drops in expression while others display stark upregulation. Previous work from the laboratory of Tony Wyss-Coray has shown that the plasma proteome exhibits peak differential expression at the ages of 34, 60, and 78.⁴ In our prior transcriptomic study, we found that human transcriptomes become dysregulated around 70 years of age.¹⁷ The gene expression-relevant methylome analogously

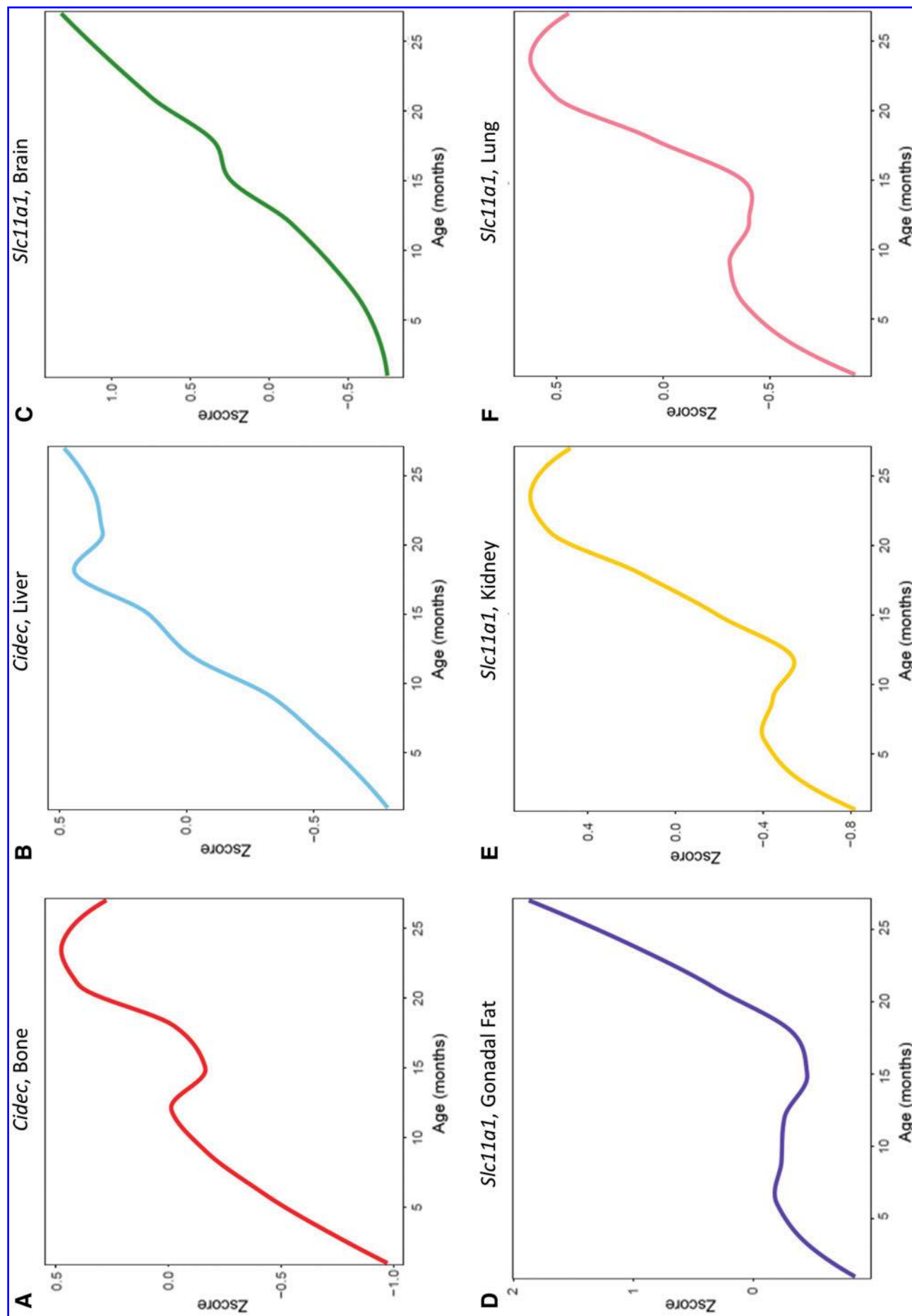


FIG. 3. *Cidec* and *Slc11a1* increase their expression level with age in different mouse tissues. *Cidec* increases with age in bone (A) and liver (B), while *Slc11a1* becomes upregulated with age in brain (C), gonadal fat (D), kidney (E), and lung (F). For all six plots (A–F), the FDR value is less than 0.05 for this age comparison. Using the Tabula Muris Senis dataset, age comparisons were made between 24-month-old age mice and 3-month-old mice. Color images are available online.

TABLE 3. THE SIX CLOCK INPUTS LISTED IN TABLE 1 WERE EXAMINED IN THE TABULA MURIS SENIS TRANSCRIPTOMIC DATASET

Gene name	Expression change with age in mouse tissue
<i>Chi3l2</i>	Not measured
<i>Cidec</i>	Bone (↑), liver (↑)
<i>Fcgr3a</i>	Not measured
<i>Rps4y1</i>	Not measured
<i>Slc11a1</i>	Brain (↑), gonadal fat (↑), kidney (↑), lung (↑)
<i>Vtn1</i>	Nonsignificant

In this multitissue mouse dataset, expression was compared between elderly mice aged 24 months and young adult mice aged 3 months. While *Chi3l2*, *Fcgr3a*, and *Rps4y1* were not available for measurement under these names, the genes *Cidec*, *Slc11a1*, and *Vtn1* were all measured in various tissues. A demarcation of ↑ or ↓, respectively, indicates that a gene is significantly (FDR <0.05) increased or decreased in a given tissue.

FDR, false discovery rate.

becomes more variable with age.⁶³ Since certain mutations can affect gene expression, it is also worthwhile to mention that somatic mutations continuously accrue with age.^{64,65} These data collectively highlight the relationship between aging and the destabilization of gene and protein expression.

Our results also indicate that, in addition to being useful for age prediction, these six clock inputs change their expression level with age in mammals and have palpable connections to age-related disease. Their connection to mul-

TABLE 4. HOW THE EXPRESSION OF THE SIX PAN-TISSUE CLOCK GENES CHANGES WITH AGE IN HUMAN BLOOD, BRAIN, OR RETINA WAS INVESTIGATED

Gene name	Expression change with age in human tissue
<i>CHI3L2</i>	Blood (↓), brain (↑), retina (↑)
<i>CIDEc</i>	Nonsignificant
<i>FCGR3A</i>	Brain (↑)
<i>RPS4Y1</i>	Nonsignificant
<i>SLC11A1</i>	Blood (↓), brain (↑)
<i>VTCN1</i>	Brain (↓)

The differential gene expression analysis was done by comparing individuals aged ≥70 years to adults in the 30–69 year age range. A demarcation of ↑ or ↓, respectively, indicates that a gene is significantly (FDR <0.05) increased or decreased in a given tissue.

iple aspects of aging indicates that their ability to contribute to a robust aging clock model is not arbitrary. Instead, they may play an active role in regulating the aging process. For example, we show that the gene *CHI3L2* is upregulated with age in the human brain and retina and has been reported to be overexpressed in both amyotrophic lateral sclerosis⁵³ and Alzheimer's disease⁵⁴ patients. Since treating mice with recombinant CHI3L2 induces arthritis⁴² and the expression of this gene positively correlates with metastasis in a subset of breast cancer patients,⁶⁶ interventions which decrease the expression level of CHI3L2 in certain tissues may prove beneficial. Another example is *VTCN1*, which has been shown to be a driver of various age-related cancers in mice.^{46,51,52} Thus, treatments that decrease the expression level of *VTCN1* may prove useful for the suppression of cancer. Supportive of this, treating human endometrial cancer cells with metformin decreases the expression of *VTCN1*.⁶⁷ This is intriguing given that metformin is an antiaging drug that increases health span in mice.⁶⁸ Another input of interest is *SLC11A1*, which increases with age in both mouse and human brain tissue. Since mice harboring a nonfunctional version of *Slc11a1* are unable to efficiently clear human alpha-synuclein oligomers,⁶⁹ the increased expression of this gene in brain tissue may reflect a defensive response to aging-associated damage. Additional research is needed to better understand the biological significance of these inputs increasing or decreasing with age in a given tissue.

One unexpected finding in this study was that six microRNAs—MIR100, MIR10B, MIR191, MIR21, MIR222, and MIR27B—underwent significant expression changes with age in human blood, brain, heart, and retina tissue. In addition to being well-established that microRNAs become differentially expressed with age^{19,70} and age-related disease,^{71,72} some microRNAs are powerful regulators of life span in animal models.^{40,41} For example, life span in worms is extended by overexpressing the microRNA lin-4.⁷³ Although MIR100, MIR191, MIR21, MIR222, and MIR27B were differentially increased or decreased with age depending on the tissue, MIR10B was consistently decreased in all four human tissues. Since a considerable body of data has linked MIR10B with cancer metastasis,⁷⁴ this microRNA may be an interesting drug target for age-related disease. The remaining microRNAs MIR100, MIR191, MIR21, MIR222, and MIR27B have been identified in conjunction with hepatocellular carcinoma cancer stem cells,⁷⁵ neurotoxicity,⁷⁶ glioma,⁷⁷ degenerative heart disease,⁷⁸ and

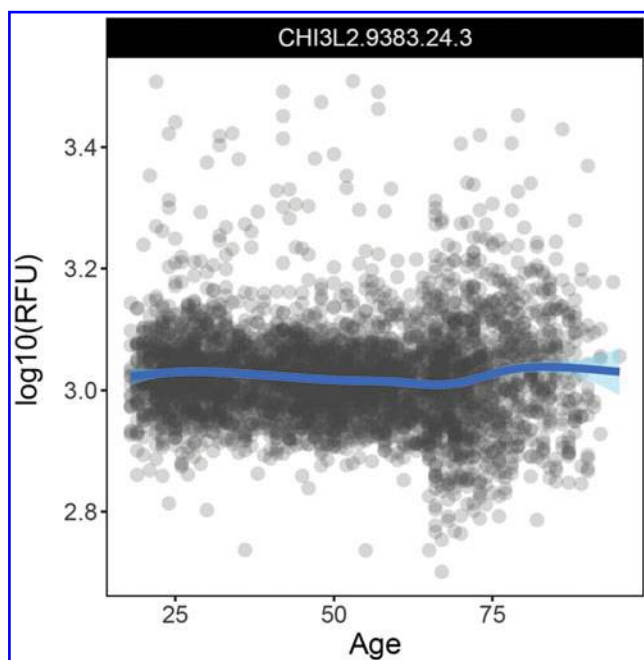


FIG. 4. *CHI3L2* becomes destabilized with age in human plasma. In a plasma proteomic dataset derived from 4263 healthy individuals aged 18–95 years, the expression level of *CHI3L2* is visualized as a function of age. *CHI3L2* significantly ($q_{\text{Age}} < 0.05$) changes its expression level with age and has a negative age coefficient. This dataset was generated using the SOMAscan assay and originates from both the INTERVAL ($n = 3301$) and LonGenity ($n = 962$) cohorts. RFU, relative fluorescence unit. Color images are available online.

TABLE 5. FOR EACH OF THE GENES LISTED IN TABLE 1, FIVE LITERATURE CONNECTIONS RELEVANT TO AGE-RELATED DISEASE ARE PROVIDED

Gene name	Literature connections relevant to age-related disease
<i>CHI3L2</i>	<p>Treating mice with recombinant <i>CHI3L2</i> induces arthritis⁴²</p> <p>The expression level of <i>CHI3L2</i> in the motor cortex is elevated in patients with amyotrophic lateral sclerosis⁵³</p> <p>Cancer-free survival in shortened and tumor relapse risk is elevated in small renal cell carcinoma patients with <i>CHI3L2</i> positive tumors⁵⁷</p> <p>A panel of five hub genes—<i>CHI3L2</i>, <i>FSTL3</i>, <i>RPA3</i>, <i>RRM2</i>, and <i>YTHDF2</i>—can be utilized to predict prognosis in patients with glioblastoma multiforme⁵⁸</p> <p><i>CHI3L2</i> in the brain is increased in Alzheimer's disease patients compared to healthy controls⁵⁴</p>
<i>CIDECD</i>	<p>Mice lacking <i>Cidec</i> are protected against diet-induced insulin resistance and weight gain⁴³</p> <p>In a genetic mouse model of diabetes, creating a deficiency in <i>Cidec</i> ameliorates obesity and enhances insulin sensitivity⁴⁷</p> <p>In a mouse model of atherosclerosis, silencing <i>Cidec</i> decreases weight gain, attenuates visceral adiposity, and shrinks the size of atherosclerotic lesions⁴⁸</p> <p>In a rat model of diabetic cardiomyopathy, silencing <i>Cidec</i> improves cardiac function and attenuates cardiac fibrosis⁴⁴</p> <p>A methylation locus in <i>CIDECD</i> is associated with inflammation in gout patients⁸⁶</p>
<i>FCGR3A</i>	<p>Genetic variants of <i>FCGR3A</i> are associated with coronary artery disease⁸⁷</p> <p>Deleting <i>Fcgr3a</i> inhibits the progression of atherosclerotic lesions in a mouse model of atherosclerosis⁴⁵</p> <p>In polymorphonuclear neutrophils derived from elderly subjects, the expression level of <i>FCGR3A</i> is elevated following hip fracture surgery⁸⁸</p> <p>A polymorphism in <i>FCGR3A</i> predicts efficacy of the drug trastuzumab in patients with ERBB2/HER2-positive breast cancer⁸⁹</p> <p>The downregulation of <i>FCGR3A</i> correlates with improved survival in patients with oral squamous cell carcinoma⁵⁹</p>
<i>RPS4Y1</i>	<p>The expression level of <i>RPS4Y1</i> is elevated in nondemented individuals with a high neurofibrillary tangle burden⁹⁰</p> <p>In peripheral blood derived from individuals with Parkinson's disease, the most upregulated gene is <i>RPS4Y1</i>⁵⁵</p> <p>A bioinformatics analysis identified <i>RPS4Y1</i> as a hub gene in patients with intervertebral disc degeneration⁹¹</p> <p>Patients with mild cognitive impairment exhibit an elevated expression level of <i>RPS4Y1</i>⁵⁶</p> <p>The gene <i>RPS4Y1</i> is frequently upregulated in heart failure patients⁹²</p>

(continued)

TABLE 5. (CONTINUED)

Gene name	Literature connections relevant to age-related disease
<i>SLC11A1</i>	<p>Cutaneous wound healing is delayed in mice lacking <i>Slc11a1</i>⁴⁹</p> <p>Chemically-induced arthritis is exacerbated in mice by introducing a mutation in <i>Slc11a1</i>⁵⁰</p> <p>Relevant to Parkinson's disease, mice harboring a nonfunctional version of <i>Slc11a1</i> display an impaired ability to degrade human alpha-synuclein oligomers⁶⁹</p> <p><i>SLC11A1</i> and three other genes can be utilized to construct a model that predicts prognosis in patients with thyroid cancer⁶⁰</p> <p>A prognostic signature that includes <i>SLC11A1</i> and five other inputs can predict prognosis in hepatocellular carcinoma patients⁶¹</p>
<i>VTCN1</i>	<p>In prostate cancer tissue, a higher expression level of <i>VTCN1</i> correlates with an elevated risk of cancer recurrence and a higher likelihood of cancer-specific death⁶²</p> <p>Mice lacking <i>Vtcn1</i> have fewer tumor modules and exhibit superior survival in mouse model of breast cancer⁴⁶</p> <p>In a mouse model of ovarian cancer, treating mice with an anti-<i>VTCN1</i> antibody delays tumor growth⁵¹</p> <p>Using siRNA to knockdown <i>VTCN1</i> in a mouse xenograft model of hepatocellular carcinoma suppresses tumor growth⁵²</p> <p>In human endometrial cancer cells, treatment with metformin decreases the expression of <i>VTCN1</i>⁶⁷</p>

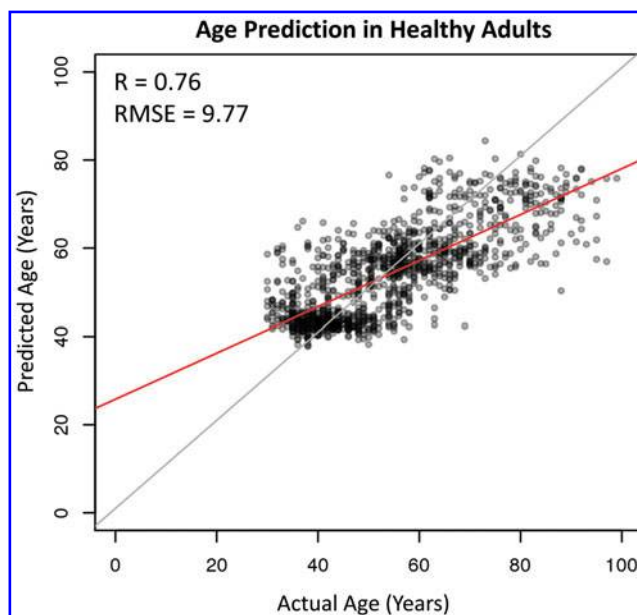


FIG. 5. A minimalistic transcriptomic aging clock. Using random forest machine learning, a 10-fold cross-validation approach was used to predict age in a large, multitissue transcriptomic dataset derived from adults aged 30–99 years. The only inputs for this clock were the genes *CHI3L2*, *CIDECD*, *FCGR3A*, *RPS4Y1*, *SLC11A1*, and *VTCN1*. This clock had a R value of 0.76 and a RMSE of 9.77 years. RMSE, root-mean square error. Color images are available online.

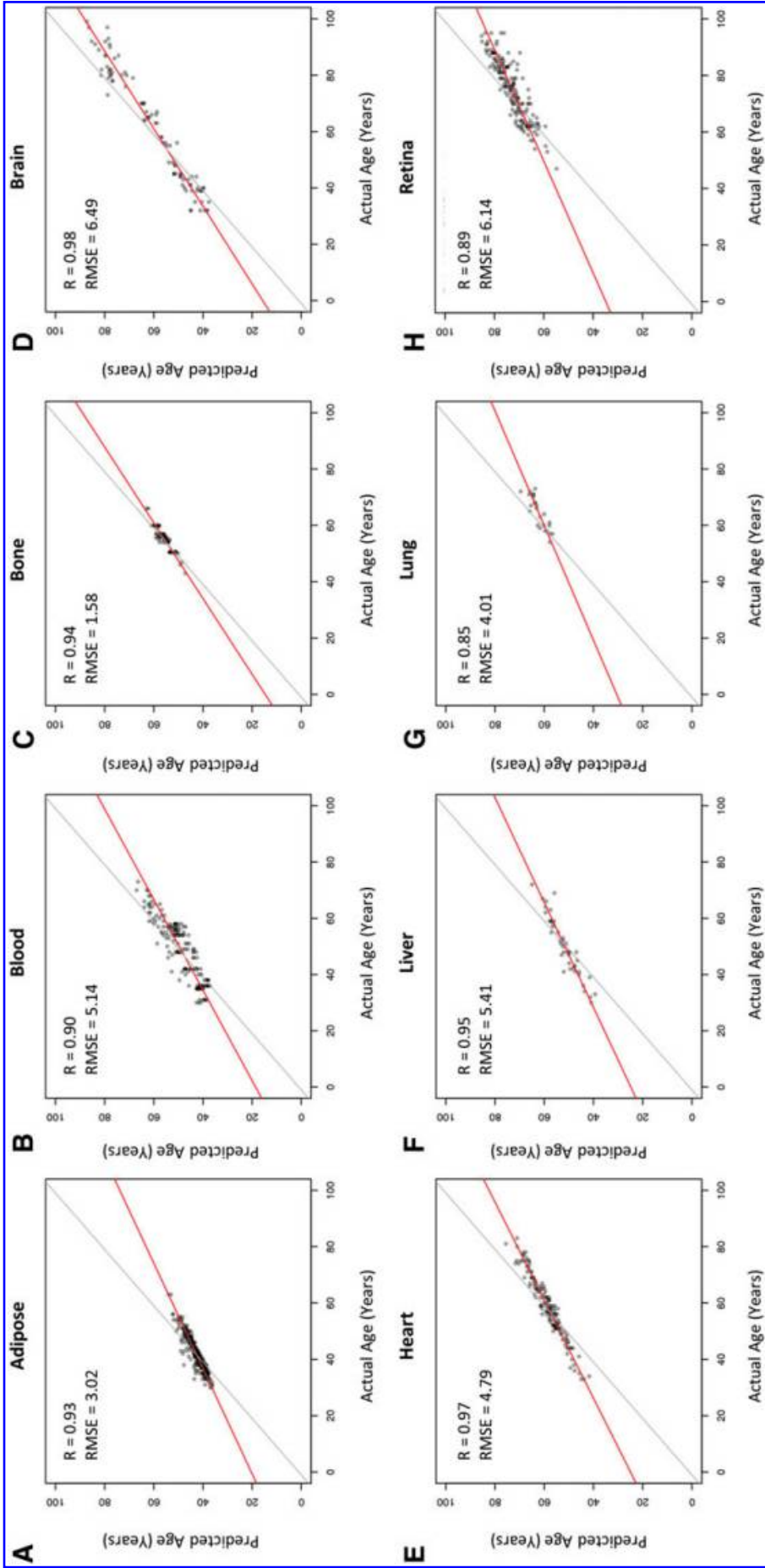


FIG. 6. Accuracy metrics across eight different tissues. Using the same large transcriptomic dataset, we show the accuracy of the clock generated in Figure 5 in adipose (A), blood (B), bone (C), brain (D), heart (E), liver (F), lung (G), and retina (H) samples. Plots visualizing predicted age versus actual age are shown for adipose ($n=374$), blood ($n=178$), bone ($n=89$), brain ($n=91$), heart ($n=151$), liver ($n=44$), lung ($n=25$), and retina ($n=176$) tissues. Color images are available online.

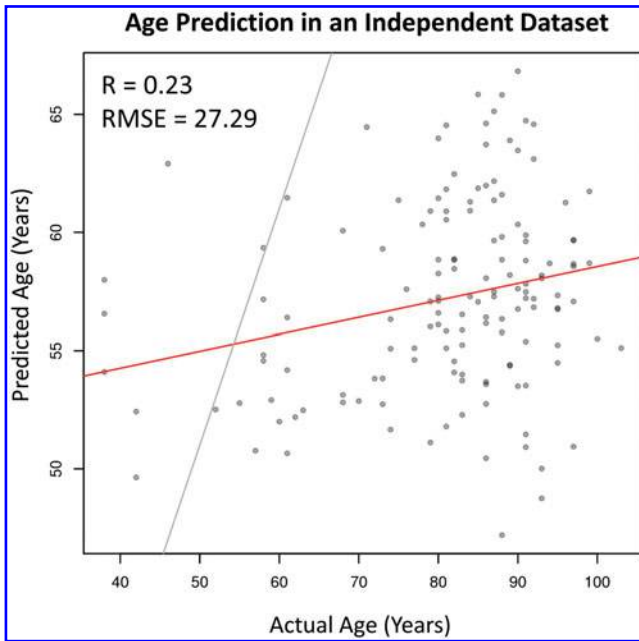


FIG. 7. Clock testing in an independent dataset. Using the clock generated in Figure 5, we predicted age in an independent RNA-seq dataset derived from human brain tissue ($n=144$, age range=38–103 years). This model was significantly correlated with age (p -value=0.0036), had a Pearson correlation of 0.23, and a RMSE of 27.29 years. Color images are available online.

osteoarthritis,⁷⁹ respectively. It would be intriguing to assess the ability of these microRNAs to impact aging in older animals.

In summary, we demonstrate that these six clock inputs are collectively enriched in immune processes, exhibit significant expression changes with age in mammalian tissue, have intimate connections to age-related disease in the literature, and can be utilized to generate a minimalistic age predictor. Future studies are warranted to better understand the relationship of these genes to age-related disease and longevity.

Methods

Over-representation and network topology-based enrichment analyses

Enrichment analyses were performed similarly to before.⁸⁰ The over-representation analysis in the Gene Ontology Biological Process database was performed using WebGestalt⁸¹ using UniProt IDs⁸² as inputs. The minimum number of genes for a category was set to three, the maximum number of genes for a category was set to 1000, and the top 10 results were identified. For the network topology-based analysis, UniProt IDs were uploaded and analyzed in the PPI BioGRID functional database³⁶ using WebGestalt. The network construction method was network expansion, and the set number of top ranking neighbors was equivalent to 50. The significance level was set to FDR=0.05, and neighbors were highlighted.

Annotations in the gene ontology database

To identify a complete list of annotations for each clock input, the gene name for each input was analyzed in the

Gene Ontology database using the following link: <http://geneontology.org/>. All duplicate annotations were removed so that only unique annotations were listed.

Measuring protein expression with age in a large plasma proteomic dataset

Previously, Lehallier et al. measured how the expression of 2925 proteins varies with age in a plasma proteomic dataset derived from 4263 healthy individuals aged 18–95 years.⁴ This dataset represents individuals from both INTERVAL ($n=3301$) and LonGenity ($n=962$) cohorts.⁴ The expression information for each of these protein measurements can be found using the following online software tool provided by Lehallier et al: https://twc-stanford.shinyapps.io/aging_plasma_proteome/. As we have done before,⁸⁰ we used this tool to look up the gene name of each of the clock inputs discussed in the present study. We also used this tool to generate a graph of CHI3L2 that shows how the expression of this protein varies with age in human plasma. “Loess” was selected as the regression line, and “All” was selected as the subset for visualization. The significance threshold was a q .Age of 0.05 or lower.

Measuring gene expression with age in different mouse organs

Gene expression in mice was assessed in the Tabula Muris Senis dataset.³⁹ Specifically, whether or not gene expression varied with mouse age in bone, brain, brown fat, gonadal fat, heart, kidney, limb muscle, liver, lung, marrow, mesenteric fat, pancreas, skin, small intestine, spleen, subcutaneous fat, or white blood cells was investigated using the following online tool created by Schaum et al.³⁹: <https://twc-stanford.shinyapps.io/macaf/>. For the bulk RNA-seq gene expression comparison, elderly mice aged 24 months were compared to young adult mice aged 3 months. Graphs of clock inputs that significantly change their expression level with age were generated using the “Trajectories” tab of this online tool. A gene was considered to significantly change its expression level with age if it had a FDR value less than 0.05.

Measuring gene expression with age in different human tissues

Using human transcriptomic data that we previously collated,¹⁷ we performed differential gene expression analyses between older adults (≥ 70 years) and younger adults (30–69 years) in blood ($n=178$, age range=30–73 years), brain ($n=91$, age range=32–99 years), heart ($n=151$, age range=33–83 years), and retina ($n=176$, age range=47–95 years) tissue. For each measured gene, the logFC, logCPM, F-score, p -value, and FDR are reported. A gene was considered to significantly change its expression level with age if it had a FDR value <0.05 . Genes that were commonly differentially expressed across different tissues were identified using the following Multiple List Comparator tool: www.molbiotools.com/listcompare.html. The human transcriptomic data analyzed are part of a larger dataset we previously collated, filtered, and made publicly available on Mendeley Data: <https://data.mendeley.com/datasets/92rgnswtn8/1>

Literature search for connections relevant to age-related disease

Gene and/or protein names were used in conjunction with PubMed (<https://pubmed.ncbi.nlm.nih.gov/>) and/or PMC (<https://www.ncbi.nlm.nih.gov/pmc/>) to search for literature connections relevant to age-related disease. Primary and alternative names for the six pan-tissue aging clock inputs were identified using UniProt.⁸²

Using random forest machine learning to generate a novel transcriptomic aging clock

As we have done previously,¹⁷ we used random forest machine learning to predict age in a transcriptomic dataset using a 10-fold cross-validation approach. The genes *CHI3L2*, *CIDEA*, *FCGR3A*, *RPS4Y1*, *SLC11A1*, and *VTCN1* were used as model inputs. Age was predicted in a multitissue dataset derived from 1225 adults spanning an age range of 30–99 years. The transcriptomes analyzed are part of the following larger dataset that we previously organized, filtered, and made available¹⁷: <https://data.mendeley.com/datasets/92rgnswtn8/1A> cutoff of 30 years was manually imposed to avoid any confounding effects of development.

To test the ability of this clock to predict age in an independent dataset, we collated publicly available RNA-Seq data generated from brain tissue.^{83–85} After applying filters and removing samples associated with disease, we were left with 144 transcriptomes spanning an age range of 38–103 years.

Acknowledgments

Both authors express gratitude to J.L., E.S., B.S., J.M., and Y.S.

Author Disclosure Statement

No competing financial interests exist.

Funding Information

Although this work did not receive any financial support, M.N.S. is grateful to funding from NIH R01 GM102491-07, NCI P30 CA014195-46, NIA 1RF1AG064049-01, NIH/NCI P30AG068635, and the Helmsley Trust.

Supplementary Material

Supplementary Table S1
Supplementary Table S2
Supplementary Table S3
Supplementary Table S4
Supplementary Table S5

References

- Horvath S. DNA methylation age of human tissues and cell types. *Genome Biol* 2013;14:R115.
- Hannum G, Guinney J, Zhao L, et al. Genome-wide methylation profiles reveal quantitative views of human aging rates. *Mol Cell* 2013;49:359–367.
- Galkin F, Mamoshina P, Aliper A, et al. Biohorology and biomarkers of aging: Current state-of-the-art, challenges and opportunities. *Ageing Res Rev* 2020;60:101050.
- Lehallier B, Gate D, Schaum N, et al. Undulating changes in human plasma proteome profiles across the lifespan. *Nat Med* 2019;25:1843–1850.
- Liu Z, Kuo PL, Horvath S, et al. A new aging measure captures morbidity and mortality risk across diverse subpopulations from NHANES IV: A cohort study. *PLoS Med* 2018;15:e1002718.
- Lehallier B, Shokhirev MN, Wyss-Coray T, Johnson AA. Data mining of human plasma proteins generates a multitude of highly predictive aging clocks that reflect different aspects of aging. *Aging Cell* 2020;19:e13256.
- Lei MK, Beach SR, Dogan MV, Philibert RA. A pilot investigation of the impact of smoking cessation on biological age. *Am J Addict* 2017;26:129–135.
- Kim S, Fuselier J, Welsh DA, et al. Feature selection algorithms enhance the accuracy of frailty indexes as measures of biological age. *J Gerontol A Biol Sci Med Sci* 2021;76:1347–1355.
- Jazwinski SM, Kim S. Examination of the dimensions of biological age. *Front Genet* 2019;10:263.
- Elliott ML, Caspi A, Houts RM, et al. Disparities in the pace of biological aging among midlife adults of the same chronological age have implications for future frailty risk and policy. *Nat Aging* 2021;1:295–308.
- Melzer D, Pilling LC, Ferrucci L. The genetics of human ageing. *Nat Rev Genet* 2020;21:88–101.
- Rexbye H, Petersen I, Johansens M, et al. Influence of environmental factors on facial ageing. *Age Ageing* 2006;35:110–115.
- Garatachea N, Pareja-Galeano H, Sanchis-Gomar F, et al. Exercise attenuates the major hallmarks of aging. *Rejuvenation Res* 2015;18:57–89.
- Tarkhov AE, Alla R, Ayyadevara S, et al. A universal transcriptomic signature of age reveals the temporal scaling of *Caenorhabditis elegans* aging trajectories. *Sci Rep* 2019;9:7368.
- Schultz MB, Kane AE, Mitchell SJ, et al. Age and life expectancy clocks based on machine learning analysis of mouse frailty. *Nat Commun* 2020;11:4618.
- Fahy GM, Brooke RT, Watson JP, et al. Reversal of epigenetic aging and immunosenescent trends in humans. *Aging Cell* 2019;18:e13028.
- Shokhirev MN, Johnson AA. Modeling the human aging transcriptome across tissues, health status, and sex. *Aging Cell* 2021;20:e13280.
- LaRocca TJ, Cavalier AN, Wahl D. Repetitive elements as a transcriptomic marker of aging: Evidence in multiple datasets and models. *Aging Cell* 2020;19:e13167.
- Huan T, Chen G, Liu C, et al. Age-associated microRNA expression in human peripheral blood is associated with all-cause mortality and age-related traits. *Aging Cell* 2018;17:e12687.
- Zhang B, Podolskiy DI, Mariotti M, et al. Systematic age-, organ-, and diet-associated ionome remodeling and the development of ionomic aging clocks. *Aging Cell* 2020;19:e13119.
- Robinson O, Chadeau Hyam M, Karaman I, et al. Determinants of accelerated metabolomic and epigenetic aging in a UK cohort. *Aging Cell* 2020;19:e13149.
- Bobrov E, Georgievskaya A, Kiselev K, et al. PhotoAge-Clock: Deep learning algorithms for development of

- non-invasive visual biomarkers of aging. *Aging* (Albany NY) 2018;10:3249–3259.
23. Bell CG, Lowe R, Adams PD, et al. DNA methylation aging clocks: Challenges and recommendations. *Genome Biol* 2019;20:249.
 24. Johnson AA, Stolzing A. The role of lipid metabolism in aging, lifespan regulation, and age-related disease. *Aging Cell* 2019;18:e13048.
 25. Chen FJ, Yin Y, Chua BT, Li P. CIDE family proteins control lipid homeostasis and the development of metabolic diseases. *Traffic* 2020;21:94–105.
 26. Romee R, Foley B, Lenvik T, et al. NK cell CD16 surface expression and function is regulated by a disintegrin and metalloprotease-17 (ADAM17). *Blood* 2013;121:3599–3608.
 27. Chaum E, Winborn CS, Bhattacharya S. Genomic regulation of senescence and innate immunity signaling in the retinal pigment epithelium. *Mamm Genome* 2015;26:210–221.
 28. Miyatake K, Tsuji K, Yamaga M, et al. Human YKL39 (chitinase 3-like protein 2), an osteoarthritis-associated gene, enhances proliferation and type II collagen expression in ATDC5 cells. *Biochem Biophys Res Commun* 2013;431:52–57.
 29. Xiao C, Sun T, Yang Z, et al. Transcriptome landscapes of differentially expressed genes related to fat deposits in Nandan-Yao chicken. *Funct Integr Genomics* 2021;21:113–124.
 30. Chang R, Chen L, Su G, et al. Identification of Ribosomal Protein S4, Y-Linked 1 as a cyclosporin A plus corticosteroid resistance gene. *J Autoimmun* 2020;112:102465.
 31. Blackwell JM, Goswami T, Evans CA, et al. SLC11A1 (formerly NRAMP1) and disease resistance. *Cell Microbiol* 2001;3:773–784.
 32. Li X, Zhang B, Wang H, et al. The effect of aging on the biological and immunological characteristics of periodontal ligament stem cells. *Stem Cell Res Ther* 2020;11:326.
 33. Sica GL, Choi IH, Zhu G, et al. B7-H4, a molecule of the B7 family, negatively regulates T cell immunity. *Immunity* 2003;18:849–861.
 34. John P, Wei Y, Liu W, et al. The B7x immune checkpoint pathway: From discovery to clinical trial. *Trends Pharmacol Sci* 2019;40:883–896.
 35. The Gene Ontology C. The gene ontology resource: 20 years and still GOing strong. *Nucleic Acids Res* 2019;47(D1):D330–D338.
 36. Oughtred R, Rust J, Chang C, et al. The BioGRID database: A comprehensive biomedical resource of curated protein, genetic, and chemical interactions. *Protein Sci* 2021;30:187–200.
 37. Rosales C, Uribe-Querol E. Phagocytosis: A fundamental process in immunity. *Biomed Res Int* 2017;2017:9042851.
 38. Lopez-Otin C, Blasco MA, Partridge L, et al. The hallmarks of aging. *Cell* 2013;153:1194–1217.
 39. Schaum N, Lehallier B, Hahn O, et al. Ageing hallmarks exhibit organ-specific temporal signatures. *Nature* 2020;583:596–602.
 40. Boehm M, Slack FJ. MicroRNA control of lifespan and metabolism. *Cell Cycle* 2006;5:837–840.
 41. Smith-Vikos T, Slack FJ. MicroRNAs and their roles in aging. *J Cell Sci* 2012;125(Pt 1):7–17.
 42. Sakata M, Masuko-Hongo K, Tsuruha J, et al. YKL-39, a human cartilage-related protein, induces arthritis in mice. *Clin Exp Rheumatol* 2002;20:343–350.
 43. Nishino N, Tamori Y, Tateya S, et al. FSP27 contributes to efficient energy storage in murine white adipocytes by promoting the formation of unilocular lipid droplets. *J Clin Invest* 2008;118:2808–2821.
 44. Zhou HM, Ti Y, Wang H, et al. Cell death-inducing DFFA-like effector C/CIDEc gene silencing alleviates diabetic cardiomyopathy via upregulating AMPKa phosphorylation. *FASEB J* 2021;35:e21504.
 45. Kelly JA, Griffin ME, Fava RA, et al. Inhibition of arterial lesion progression in CD16-deficient mice: Evidence for altered immunity and the role of IL-10. *Cardiovasc Res* 2010;85:224–231.
 46. Abadi YM, Jeon H, Ohaegbulam KC, et al. Host b7x promotes pulmonary metastasis of breast cancer. *J Immunol* 2013;190:3806–3814.
 47. Toh SY, Gong J, Du G, et al. Up-regulation of mitochondrial activity and acquirement of brown adipose tissue-like property in the white adipose tissue of fsp27 deficient mice. *PLoS One* 2008;3:e2890.
 48. Rajamoorthi A, Lee RG, Baldan A. Therapeutic silencing of FSP27 reduces the progression of atherosclerosis in Ldlr(-/-) mice. *Atherosclerosis* 2018;275:43–49.
 49. Thuraingam T, Sam H, Moisan J, et al. Delayed cutaneous wound healing in mice lacking solute carrier 11a1 (formerly Nramp1): Correlation with decreased expression of secretory leukocyte protease inhibitor. *J Invest Dermatol* 2006;126:890–901.
 50. Peters LC, Jensen JR, Borrego A, et al. Slc11a1 (formerly NRAMP1) gene modulates both acute inflammatory reactions and pristane-induced arthritis in mice. *Genes Immun* 2007;8:51–56.
 51. Dangaj D, Lanitis E, Zhao A, et al. Novel recombinant human b7-h4 antibodies overcome tumoral immune escape to potentiate T-cell antitumor responses. *Cancer Res* 2013;73:4820–4829.
 52. Dong L, Xie L, Li M, et al. Downregulation of B7-H4 suppresses tumor progression of hepatocellular carcinoma. *Sci Rep* 2019;9:14854.
 53. Sanfilippo C, Longo A, Lazzara F, et al. CHI3L1 and CHI3L2 overexpression in motor cortex and spinal cord of sALS patients. *Mol Cell Neurosci* 2017;85:162–169.
 54. Sanfilippo C, Castrogiovanni P, Imbesi R, Di Rosa M. CHI3L2 expression levels are correlated with AIF1, PECAM1, and CALB1 in the brains of Alzheimer's disease patients. *J Mol Neurosci* 2020;70:1598–1610.
 55. Sakharkar MK, Kashmir Singh SK, Rajamanickam K, et al. A systems biology approach towards the identification of candidate therapeutic genes and potential biomarkers for Parkinson's disease. *PLoS One* 2019;14:e0220995.
 56. Fernandez-Martinez JL, Alvarez-Machancoses O, de Andres-Galiana EJ, et al. Robust sampling of defective pathways in Alzheimer's disease. Implications in drug repositioning. *Int J Mol Sci* 2020;21:3594.
 57. Pusztai C, Yusenko MV, Banyai D, et al. M2 macrophage marker chitinase 3-like 2 (CHI3L2) associates with progression of conventional renal cell carcinoma. *Anticancer Res* 2019;39:6939–6943.
 58. Du J, Yan X, Mi S, et al. Identification of prognostic model and biomarkers for cancer stem cell characteristics in glioblastoma by network analysis of multi-omics data and stemness indices. *Front Cell Dev Biol* 2020;8:558961.
 59. Elahi M, Rakhshan V. MED15, transforming growth factor beta 1 (TGF-beta1), FcgammaRIII (CD16), and HNK-1

- (CD57) are prognostic biomarkers of oral squamous cell carcinoma. *Sci Rep* 2020;10:8475.
60. Zhuang G, Zeng Y, Tang Q, et al. Identifying M1 macrophage-related genes through a co-expression network to construct a four-gene risk-scoring model for predicting thyroid cancer prognosis. *Front Genet* 2020;11:591079.
 61. Zhu P, Li FF, Zeng J, et al. Integrative analysis of the characteristics of lipid metabolism-related genes as prognostic prediction markers for hepatocellular carcinoma. *Eur Rev Med Pharmacol Sci* 2021;25:116–126.
 62. Zang X, Thompson RH, Al-Ahmadie HA, et al. B7-H3 and B7x are highly expressed in human prostate cancer and associated with disease spread and poor outcome. *Proc Natl Acad Sci U S A* 2007;104:19458–19463.
 63. Sliker RC, van Itersen M, Luijk R, et al. Age-related accrual of methylomic variability is linked to fundamental ageing mechanisms. *Genome Biol* 2016;17:191.
 64. Lodato MA, Rodin RE, Bohrsen CL, et al. Aging and neurodegeneration are associated with increased mutations in single human neurons. *Science* 2018;359:555–559.
 65. Milholland B, Auton A, Suh Y, Vijg J. Age-related somatic mutations in the cancer genome. *Oncotarget* 2015;6:24627–24635.
 66. Liu T, Larionova I, Litviakov N, et al. Tumor-associated macrophages in human breast cancer produce new monocyte attracting and pro-angiogenic factor YKL-39 indicative for increased metastasis after neoadjuvant chemotherapy. *Oncoimmunology* 2018;7:e1436922.
 67. Lange C, Machado Weber A, Schmidt R, et al. Changes in protein expression due to metformin treatment and hyperinsulinemia in a human endometrial cancer cell line. *PLoS One* 2021;16:e0248103.
 68. Martin-Montalvo A, Mercken EM, Mitchell SJ, et al. Metformin improves healthspan and lifespan in mice. *Nat Commun* 2013;4:2192.
 69. Wu KC, Liou HH, Kao YH, et al. The critical role of Nramp1 in degrading alpha-synuclein oligomers in microglia under iron overload condition. *Neurobiol Dis* 2017;104:61–72.
 70. Noren Hooten N, Fitzpatrick M, Wood WH, 3rd, et al. Age-related changes in microRNA levels in serum. *Aging (Albany, NY)* 2013;5:725–740.
 71. Wallenborn M, Xu LX, Kirsten H, et al. Molecular analyses of glioblastoma stem-like cells and glioblastoma tissue. *PLoS One* 2020;15:e0234986.
 72. Cogswell JP, Ward J, Taylor IA, et al. Identification of miRNA changes in Alzheimer's disease brain and CSF yields putative biomarkers and insights into disease pathways. *J Alzheimers Dis* 2008;14:27–41.
 73. Boehm M, Slack F. A developmental timing microRNA and its target regulate life span in *C. elegans*. *Science* 2005;310:1954–1957.
 74. Sheedy P, Medarova Z. The fundamental role of miR-10b in metastatic cancer. *Am J Cancer Res* 2018;8:1674–1688.
 75. Seol HS, Akiyama Y, Lee SE, et al. Loss of miR-100 and miR-125b results in cancer stem cell properties through IGF2 upregulation in hepatocellular carcinoma. *Sci Rep* 2020;10:21412.
 76. Li H, Du M, Xu W, Wang Z. MiR-191 downregulation protects against isoflurane-induced neurotoxicity through targeting BDNF. *Toxicol Mech Methods* 2021;31:367–373.
 77. Liu F, Yang B. Double-targeted knockdown of miR-21 and CXCR4 inhibits malignant glioma progression by suppression of the PI3K/AKT and Raf/MEK/ERK pathways. *Biomed Res Int* 2020;2020:7930160.
 78. Zhou H, Lin S, Li X, et al. Serum miR-222 is independently associated with atrial fibrillation in patients with degenerative valvular heart disease. *BMC Cardiovasc Disord* 2021;21:98.
 79. Li SH, Wu QF. MicroRNAs target on cartilage extracellular matrix degradation of knee osteoarthritis. *Eur Rev Med Pharmacol Sci* 2021;25:1185–1197.
 80. Johnson AA, Shokhirev MN, Wyss-Coray T, Lehallier B. Systematic review and analysis of human proteomics aging studies unveils a novel proteomic aging clock and identifies key processes that change with age. *Ageing Res Rev* 2020;60:101070.
 81. Liao Y, Wang J, Jaehnig EJ, et al. WebGestalt 2019: Gene set analysis toolkit with revamped UIs and APIs. *Nucleic Acids Res* 2019;47(W1):W199–W205.
 82. UniProt C. UniProt: A worldwide hub of protein knowledge. *Nucleic Acids Res* 2019;47(D1):D506–D515.
 83. Magistri M, Velmeshev D, Makhmutova M, Faghihi MA. Transcriptomics profiling of Alzheimer's disease reveal neurovascular defects, altered amyloid-beta homeostasis, and deregulated expression of long noncoding RNAs. *J Alzheimers Dis* 2015;48:647–665.
 84. Nativio R, Donahue G, Berson A, et al. Dysregulation of the epigenetic landscape of normal aging in Alzheimer's disease. *Nat Neurosci* 2018;21:497–505.
 85. Srinivasan K, Friedman BA, Etxeberria A, et al. Alzheimer's patient microglia exhibit enhanced aging and unique transcriptional activation. *Cell Rep* 2020;31:107843.
 86. Tseng CC, Liao WT, Wong MC, et al. Cell lineage-specific methylome and genome alterations in gout. *Aging (Albany NY)* 2021;12.
 87. Gavasso S, Nygard O, Pedersen ER, et al. Fcgamma receptor IIIA polymorphism as a risk-factor for coronary artery disease. *Atherosclerosis* 2005;180:277–282.
 88. Baehl S, Garneau H, Le Page A, et al. Altered neutrophil functions in elderly patients during a 6-month follow-up period after a hip fracture. *Exp Gerontol* 2015;65:58–68.
 89. Gavin PG, Song N, Kim SR, et al. Association of polymorphisms in FCGR2A and FCGR3A with degree of trastuzumab benefit in the adjuvant treatment of ERBB2/HER2. Positive breast cancer: analysis of the NSABP B-31 trial. *JAMA Oncol* 2017;3:335–341.
 90. Wilmot B, McWeeney SK, Nixon RR, et al. Translational gene mapping of cognitive decline. *Neurobiol Aging* 2008;29:524–541.
 91. Fan Z, Zhao W, Fan S, et al. Identification of potential biomarkers for intervertebral disc degeneration using the genome-wide expression analysis. *J Comput Biol* 2020;27:1341–1349.
 92. Jiang Z, Guo N, Hong K. A three-tiered integrative analysis of transcriptional data reveals the shared pathways related to heart failure from different aetiologies. *J Cell Mol Med* 2020;24:9085–9096.

Address correspondence to:
 Adiv A. Johnson
 Independent Researcher
 Tucson, AZ
 USA

E-mail: adivjohnson@gmail.com

Received: March 2, 2021
 Accepted: August 31, 2021